Biogenesis of MalF and the MalFGK(2) maltose transport complex in Escherichia coli requires YidC.

Wagner, S.; Pop, O.I.; Haan, G.J.; Koningstein, G.M.; Klepsch, M.M.; Genevaux, P.; Luirink, S.; de Gier, J.-W.

published in
Journal of Biological Chemistry
2008

DOI (link to publisher)
10.1074/jbc.M801481200

document version
Publisher's PDF, also known as Version of record

THE JOURNAL OF BIOLOGICAL CHEMISTRY VOL. 283, NO. 26, pp. 17881–17890, June 27, 2008

Biogenesis of MalF and the $MalFGK_2$ Maltose Transport Complex in *Escherichia coli* Requires YidC*

Received for publication, February 25, 2008, and in revised form, April 21, 2008 Published, JBC Papers in Press, May 2, 2008, DOI 10.1074/jbc.M801481200

Samuel Wagner[‡1], Ovidio Pop[§1], Gert-Jan Haan[§1,2], Louise Baars[‡], Gregory Koningstein[§], Mirjam M. Klepsch[‡], Pierre Genevaux[¶], Joen Luirink[§3], and Jan-Willem de Gier[‡4]

From the [‡]Center for Biomembrane Research, Department of Biochemistry and Biophysics, Stockholm University, Stockholm SE-106 91, Sweden, the [§]Department of Molecular Microbiology, Institute of Molecular Cell Biology, Vrije Universiteit, De Boelelaan 1085, Amsterdam 1081 HV, The Netherlands, and the [¶]Laboratoire de Microbiologie et Génétique Moléculaires, Institut de Biologie Cellulaire et de Génétique, CNRS, Université Paul-Sabatier, 118 Route de Narbonne, Toulouse 31062, Cedex 09, France

The polytopic inner membrane protein MalF is a constituent of the $MalFGK_2$ maltose transport complex in *Escherichia coli*. We have studied the biogenesis of MalF using a combination of *in vivo* and *in vitro* approaches. MalF is targeted via the SRP pathway to the Sec/YidC insertion site. Despite close proximity of nascent MalF to YidC during insertion, YidC is not required for the insertion of MalF into the membrane. However, YidC is required for the stability of MalF and the formation of the $MalFGK_2$ maltose transport complex. Our data indicate that YidC supports the folding of MalF into a stable conformation before it is incorporated into the maltose transport complex.

In the Gram-negative bacterium *Escherichia coli*, different inner membrane protein targeting and insertion pathways are operational (1). Although the biogenesis requirements of only a few membrane proteins have been studied thoroughly, most of them are targeted via the signal recognition particle (SRP)[5] pathway to the inner membrane where they are delivered at the Sec translocon (2, 3). The core of the Sec translocon consists of the integral membrane proteins SecY and SecE and the peripheral ATPase SecA (4–6). SecY and -E form a protein-conducting channel that can mediate both translocation and membrane insertion (4, 7). It has been proposed that the translocon channel can open laterally toward the lipid bilayer thereby allowing the release of transmembrane segments (TMs) into the membrane (6, 8). The ATPase SecA is required for the translocation of large (≥60 amino acids) periplasmic domains of inner membrane proteins (1, 9).

The inner membrane protein YidC, which is essential for viability, has been identified as a factor that assists in the integration, folding, and assembly of inner membrane proteins both in association with the Sec translocon and separately (10, 11). Thus far, only a handful of inner membrane proteins that insert via the YidC-only pathway have been identified. All these proteins are small and do not contain a sizable periplasmic domains and more than two TMs. It is not clear how YidC assists the biogenesis of these proteins. During the biogenesis of SRP/Sec translocon-dependent inner membrane proteins, YidC specifically interacts with the TMs of these proteins (*e.g.* Refs. 12–15). It has been suggested that YidC mediates the transfer of TMs from the Sec translocon into the lipid bilayer (1). Indeed, YidC could be co-purified with the Sec translocon, suggesting a physical connection (14). A recent *in vitro* study using lactose permease (LacY) reveals a novel function for YidC in the co-translational folding of this inner membrane protein rather than its insertion into the membrane (16). The observation that YidC depletion leads to the induction of the Cpx and σ^E envelope stress responses, which both sense protein misfolding in the cell envelope, also points to a role of YidC in the folding of inner membrane proteins (17, 18).

Here, we have used the inner membrane protein MalF as a model protein to study the role of YidC in the biogenesis of polytopic inner membrane proteins, which are part of a hetero-oligomeric complex. MalF functions in maltose transport as a 1:1:2 complex with the integral inner membrane protein MalG and the peripheral inner membrane protein MalK (19, 20). The complex belongs to the ATP-binding cassette (ABC) transporter superfamily. MalF is a 514-amino acid-long inner membrane protein containing 8 TMs, with its N and C termini facing the cytosol (21) (see Fig. 1). A large periplasmic domain (~180 amino acids) is present between the third and the fourth transmembrane segments. This domain folds into a trypsin-resistant conformation when MalF is incorporated into the $MalFGK_2$ maltose transport complex (22).

The biogenesis of MalF was studied using a combination of *in vivo* and *in vitro* approaches. MalF was found to be targeted via the SRP pathway to the Sec/YidC insertion site. Despite close proximity of nascent MalF to YidC during insertion, YidC appeared dispensable for the insertion of MalF into the membrane. However, YidC is required for the stability of MalF and the formation of the $MalFGK_2$ maltose transport complex suggesting an important role of YidC in the assembly of oligomeric complexes in the inner membrane.

* The costs of publication of this article were defrayed in part by the payment of page charges. This article must therefore be hereby marked "*advertisement*" in accordance with 18 U.S.C. Section 1734 solely to indicate this fact.
[1] These authors contributed equally to this work.
[2] Supported by EU-network Grant QLK-C-T2000-00082. Centocor B.V., Einsteinweg 92, Leiden 2333 CD, The Netherlands.
[3] To whom correspondence may be addressed. Tel.: 31-20-598-7175; Fax: 31-20-598-6979; E-mail: joen.luirink@falw.vu.nl.
[4] To whom correspondence may be addressed. Tel.: 46-8-162-420; Fax: 46-8-153-679; E-mail: degier@dbb.su.se.
[5] The abbreviations used are: SRP, signal recognition particle; TM, transmembrane; IMV, inverted membrane vesicle; IPTG, isopropyl 1-thio-β-D-galactopyranoside; TF, trigger factor; PSBT, *P. shermanii* transcarboxylase; Lep, leader peptidase.

EXPERIMENTAL PROCEDURES

Materials—Restriction endonucleases and the Expand Long Template PCR system were from Roche Molecular Biochemicals. The Megashort Script T7 transcription kit was from Ambion Inc. [^{35}S]Methionine and protein A-Sepharose were both from GE Healthcare. T4 ligase and T4 DNA polymerase were both from Epicenter Technologies. *n*-Dodecyl-β-D-maltopyranoside was from Anatrace. Serva Blue G was obtained from Serva. All other chemicals were obtained from Sigma. A polyclonal antibody against the c-Myc epitope tag was obtained from Abcam. Antisera against SecY, SecE, YidC, and Ffh were from our own collection. Antisera against MalF, -G, and -K, trigger factor (TF), and L23 were kind gifts from A. Davidson, W. Wickner, and R. Brimacombe, respectively.

In Vitro Cross-linking—E. coli strain MRE600 was used to prepare a lysate for translation of *in vitro* synthesized mRNA and suppression of UAG stop codons in the presence of (Tmd)-Phe-tRNA^{sup}. Strain MC4100 was used to isolate inverted membrane vesicles (IMVs). Strain JM110 was used to isolate pC4Meth-derived plasmids for *in vitro* transcription.

pC4Meth-derived plasmids for *in vitro* expression of truncated forms of MalF were constructed by PCR using pTAZFQ as template (23). These plasmids encode truncated MalF fused to a 4× methionine tag to improve labeling efficiency of nascent chains with [^{35}S]methionine. Immunoprecipitation of nascent chains was enabled by constructing a complementary set of constructs with a C-terminal c-Myc epitope tag (EQKLISEEDL) fused to the truncated MalF sequence. Furthermore, amber mutations (TAG) were introduced at the indicated positions to enable sup-tRNA photo-cross-linking, as described previously (14). The nucleotide sequence of all constructs was confirmed by DNA sequencing.

Truncated mRNAs were prepared from HindIII- or ClaI-linearized pC4Meth-derived plasmids. *In vitro* translation, targeting to IMVs, photo-cross-linking, carbonate extraction (to separate membrane-bound material from non-membrane-bound material), and sample processing were performed as described previously (14).

Strains, Plasmids, Growth Conditions, and Assay Used in MalF Membrane Targeting/Insertion Experiments in Vivo—The 4.5 S RNA conditional strain FF283 was cultured in M9 minimal medium (for composition, see Ref. 24) supplemented with 1 mM IPTG as described previously (24). To deplete cells of 4.5 S RNA, cells were grown to mid-log phase in the absence of IPTG. The temperature-sensitive amber suppressor SecA depletion strain BA13 and the control strain DO251 were cultured in M9 minimal medium at 30 °C, as described previously (24). To deplete cells of SecA, they were grown to mid-log phase at 41 °C. The SecE depletion strain CM124 was cultured in M9 minimal medium supplemented with 0.2% glucose and 0.2% L-arabinose as described previously (24). To deplete cells of SecE, cells were grown to mid-log phase in the absence of L-arabinose. Depletion of SecA and SecE was checked by monitoring the accumulation of pro-OmpA during a short pulse-labeling step with [^{35}S]methionine. The SecG deletion strain KN370 was cultured in M9 minimal medium to mid-log phase, and plasmid pH^+ was used to complement with SecG as described previously (24). The YidC depletion strain FTL10 was cultured in M9 minimal medium supplemented with 0.2% glucose and 0.2% L-arabinose, as described previously (25). To deplete cells of YidC, cells were grown to mid-log phase in the absence of L-arabinose.

MalF was expressed by arabinose induction from the pBAD24 vector (26) in strains FF283, BA13, DO251, and KN370 (±pH^+), by IPTG induction from the pEH1 vector (27) in strain CM124 and by IPTG induction from the pEH3 vector (27) in strain FTL10. Where appropriate, ampicillin (final concentration, 100 μg/ml), chloramphenicol (final concentration, 30 μg/ml), kanamycin (final concentration, 50 μg/ml), streptomycin (final concentration, 25 μg/ml), and tetracycline (final concentration, 12.5 μg/ml) were added to the medium.

For all experiments cells were grown to mid-log phase. Expression of the constructs was induced for 3 min with either IPTG (final concentration, 1 mM) or L-arabinose (final concentration, 0.2%). Cells were labeled with [^{35}S]methionine (100 μCi/ml, 1 Ci = 25 GBq) for 30 s. After labeling, cells were converted to spheroplasts. For spheroplasting, cells were collected at 14,000 rpm for 30 s in a microfuge, resuspended in ice-cold buffer (40% w/v sucrose, 33 mM Tris-HCl, pH 8.0), and incubated with lysozyme (final concentration, 5 μg/ml) and 1 mM EDTA for 15 min on ice. Aliquots of the spheroplast suspension were incubated on ice for 1 h either in the presence or absence of proteinase K (final concentration, 0.3 mg/ml). Subsequently, phenylmethylsulfonyl fluoride was added to the spheroplast suspension (final concentration, 0.33 mg/ml) to inhibit the protease. After addition of phenylmethylsulfonyl fluoride, samples were precipitated with trichloroacetic acid (final concentration, 10%), washed with acetone, resuspended in 10 mM Tris-HCl, pH 8.0/2% SDS, immunoprecipitated with antisera to MalF, OmpA (a periplasmic control), and AraB/bandX (a cytoplasmic control), washed, and analyzed by standard SDS-PAGE (24). Gels were scanned in a Fuji FLA-3000 phosphorimaging device and quantitated using Image Gauge (version 3.4). All pulse experiments were repeated at least three times.

For the MalF biotinylation-based membrane insertion assay, the genes encoding the MalF derivatives MalF I (MalF with a PBST biotinylation domain engineered in the periplasmic loop between TM3 and -4, Fig. 1) and MalF L (MalF with a PBST biotinylation domain engineered in the cytoplasmic loop between TM4 and -5, Fig. 1) were cloned into the expression vector pASK-IBA3 (IBA GmbH, Germany) (28). The expression vectors containing the two derivatives of MalF were transformed into the conditional YidC strain FTL10. Cells were grown overnight in LB medium containing arabinose. Cultures were then washed and transferred into fresh LB medium containing arabinose or glucose to deplete cells for YidC. Expression of MalF-I and -L was induced by addition of 0.2 μg/ml anhydrotetracycline. After 4 h samples were taken and processed for SDS-PAGE and immunoblotting. Biotinylated proteins were detected using streptavidin-horseradish peroxidase (GE Healthcare).

Analysis of the Accumulation Levels of the MalFGK$_2$ Maltose Transport Complex by Blue Native PAGE—Overnight cultures of MC4100*ara*$^+$ and FTL10 cells were grown in LB medium supplemented with 0.2% glycerol. To induce the expression of

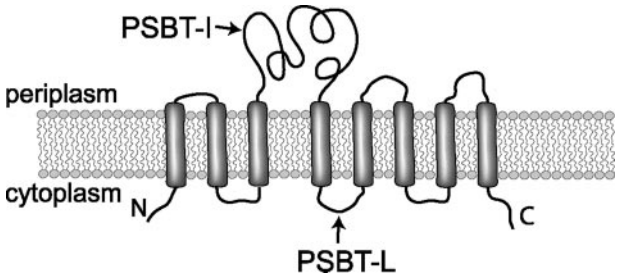

FIGURE 1. **Topology of MalF and MalF derivatives MalF-PBST I and L.** MalF contains eight TMs, and both the N and C termini face the cytosol. A large periplasmic domain (~180 amino acids) is present between the third and the fourth TMs. In MalF derivative MalF-PBST I the PSBT biotin-accepting domain from the 1.3 S subunit of *P. shermanii* transcarboxylase (*PSBT*) was engineered in the large periplasmic loop between TM3 and -4, and in the MalF derivative MalF-PBST L the PBST domain was engineered in the small cytoplasmic loop between TM4 and i5.

YidC in FTL10 during growth overnight, 0.2% arabinose was added. Cells were harvested by centrifugation and resuspended to an A_{660} of 0.05 in fresh LB medium supplemented with 0.2% glycerol and 0.2% maltose. It should be noted that the maltose transport complex is also expressed in the absence of maltose (29). After 3 h of growth, cells were collected by centrifugation and fractionated, and IMVs were isolated as described before (29). The accumulation levels of the MalFGK$_2$ maltose transport complex were analyzed by blue native-PAGE (30) followed by Western blot analysis. Sample preparation and running conditions were essentially as described previously (29). For blotting of blue native-PAGE gels, the cathode buffer containing 0.02% Serva Blue G was exchanged after one-third of the run to cathode buffer containing 0.002% Serva Blue G. This was done to prevent excessive binding of the dye to the polyvinylidene difluoride membrane. Blotting and decoration of blots with antisera to MalF, -G, -K, YidC, and SecY were performed as described previously (29).

Western Blotting Analysis—The accumulation levels of MalF, MalK, MalG, and YidC in inner membranes were monitored by immunoblot analysis. IMVs (3–5 μg of protein) were separated by standard SDS-PAGE, and immunoblotting was performed as described previously (29). To verify the specificity of the MalG signal, a *malG* deletion mutant (SW1242) was used (see below).

Construction of malG and malK Deletion Strains and FTL10 malF::Tn10—malG and *malK* deletion mutants were made using the Red Swap method (31). In brief, primers "malG_ECOLI_swapc_HP1" (5′-AACCTGAAAGCCACGCGAATGAAGTTTGATTAAGGGAGATAACAAAAATGTGTAGGCTGGAGCTGCTTCG-3′) and "malG_ECOLI_swapc_HP2" (5′-AGCGGCATAACATTGGCAGAACAACATCTTTAACCTTTCACACCACCTGCCATATGAATATCCTCCTTAG-3′) or "malK_ECOLI_swapc_HP1" (5′-TCATGAATGTTGCTGTCGATGACAGGTTGTTACAAAGGGAGAAGGGCATGTGTAGGCTGGAGCTGCTTCG-3′) and "malK_ECOLI_swapc_HP2" (5′-TGACAGGCTTTGTGTGTTTTGTGGGGTGCTTAAACGCCCGGCTCCTTATGCATATGAATATCCTCCTTAG-3′) were used to amplify the chloramphenicol resistance cassette from pKD3 (31). MC4100*ara*$^+$ harboring plasmid pKD46 (31) was grown in SOB medium (for composition, see Ref. 31) supplemented with 100 μg/ml ampicillin and 0.2% L-arabinose and used to make competent cells. After electroporation with the PCR product, chloramphenicol-resistant colonies were isolated on agar plates containing 30 μg/ml chloramphenicol. Deletion of *malG* and *malK* was verified by PCR with the following primers: k1, k2 (31), "malG_ECOLI_swap_U" (5′-CAATTGCCACGCTGATCTTC-3′), "malG_ECOLI_swap_D" (5′-CGTGACTCAGAGCACGAAAG-3′), "malK_ECOLI_swap_U" (5′-GGTGGAGGATTTAAGCCATC-3′), and "malK_ECOLI_swap_D" (5′-GCTACCTGTCCAACCAATAC-3′). Strains SW1242 (Δ*malG*) and SW1282 (Δ*malK*) were tested for defective maltose fermentation on McConkey agar plates containing 1% maltose.

The *malF::Tn10* (TetR) mutant allele (a kind gift of Michael Ehrmann, University of Duisburg-Essen, Germany) was moved into strain FTL10 by bacteriophage P1-mediated generalized transduction (32). FTL10 *malF::Tn10* (Tet^R) transductants were selected at 37 °C on LB agar plates supplemented with sodium citrate (10 mM), L-arabinose (0.1%), and tetracycline (15 μg/ml). Transductants were further tested for defective maltose fermentation on McConkey agar plates containing maltose.

Monitoring the Stability of MalF upon Depletion of YidC—Overnight cultures of MC4100ara$^+$, FTL10, SW1242, and SW1282 cells were grown in LB medium supplemented with 0.2% glycerol. To induce the expression of YidC in FTL10 during growth overnight, 0.2% arabinose was added. Cells were harvested by centrifugation and resuspended to an A_{660} of 0.05 in fresh LB medium supplemented with 0.2% glycerol. To induce the expression of YidC in FTL10, 0.2% arabinose was added. To induce the expression of the mal operon, 0.2% maltose was added. After 3 h of growth, cells were collected by centrifugation and resuspended to an A_{660} of 2.0 in 1 ml of minimal medium supplemented with all amino acids, except methionine and cysteine, and containing 0.2% glycerol and 0.2% maltose. Cells were labeled with [^{35}S]methionine for 5 min, followed by chases of 3, 30, and 60 min, and subsequently precipitated with trichloroacetic acid. Precipitated material was processed as described above under "Strains, Plasmids, Growth Conditions, and Assay Used in MalF Membrane Targeting/Insertion Experiments *in Vivo*."

RESULTS

Nascent MalF Interacts with TF, Ffh, and the Ribosomal Component L23 and Inserts into the Inner Membrane in the Vicinity of YidC and the Sec Translocon—We initially analyzed the pathway of targeting and membrane insertion of MalF using an *in vitro* translation/targeting/photo-cross-linking approach. Radiolabeled nascent MalF of 88 amino acids was synthesized in a wild-type cell-free *E. coli* extract in the presence of inverted inner membrane vesicles to allow membrane targeting and insertion on the ribosome nascent chain complex (14). At this length, the ribosome nascent chain complex is expected to fully expose the first and second TMs of MalF, assuming that the ribosome covers ~30 amino acids (33). To enable the incorporation of a photoreactive probe in the middle of the first TM of MalF, a single TAG amber codon was introduced at position 26. Following translation in the presence of (Tmd)Phe-tRNA^{sup} and UV-induced cross-linking, samples were extracted with sodium carbonate at pH 11.5 to separate membrane-integrated

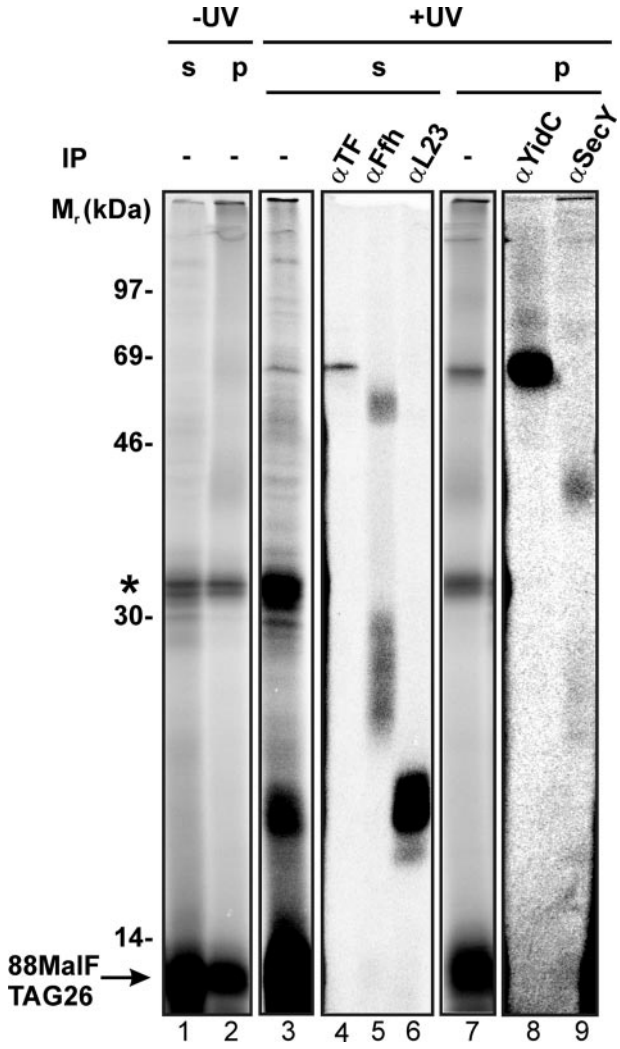

FIGURE 2. **Interactions of nascent 88MalFTAG26.** 88MalFTAG26 was synthesized *in vitro* in the presence of (Tmd)Phe-tRNA^{Sup} and *E. coli* wild-type IMVs. After translation, samples were either kept in the dark (−*UV*) or, alternatively, cross-linking was induced by UV irradiation (+*UV*). A carbonate extraction was performed to separate membrane-integrated (*p*) from soluble and peripheral membrane proteins (*s*). Immunoprecipitations were performed using the indicated antibodies. Immunoprecipitated samples and carbonate pellets and supernatants were subjected to SDS-PAGE and phosphorimaging. The position of the 88MalFTAG26 nascent chain in the gel is indicated. Peptidyl-tRNA band is marked with an *asterisk*.

from untargeted material. Cross-linked partners were identified by immunoprecipitation with specific antibodies.

The TAG26 mutation in 88MalFTAG26 was efficiently suppressed by (Tmd)Phe-tRNA^{sup} (data not shown), resulting in nascent MalF of the expected molecular weight. 88MalFTAG26 was efficiently targeted to IMVs, as judged by the relative amount of carbonate-resistant material (Fig. 2, compare *lanes 1* and *2*). Upon UV irradiation, several specific cross-linking products could be observed in the carbonate supernatant and pellet fractions (Fig. 2, *lanes 3* and *7*). An adduct of ~55 kDa could be immunoprecipitated with antiserum to Ffh, the protein component of *E. coli* SRP (Fig. 2, *lane 5*). Substantial amounts of smaller adducts were also precipitated with antiserum to Ffh, which most probably represent cross-linked degradation products of Ffh (34). A cross-linking product of ~65 kDa could be immunoprecipitated with antiserum to trigger factor (TF), which is a cytosolic chaperone with general affinity for nascent polypeptides that resides on the ribosome close to the nascent chain exit site (35, 36) (Fig. 2, *lane 4*). A prominent ~20-kDa cross-link product was precipitated with antibodies directed toward the ribosomal protein L23 (Fig. 2, *lane 6*), which is located near the nascent chain exit site (37). Ffh and TF have both been shown to associate with L23 (34, 36, 38–40). In the carbonate pellet fraction a very strong cross-linking product of ~60 kDa becomes apparent after UV irradiation (Fig. 2, *lane 7*). We could immunoprecipitate this adduct with antiserum to YidC (Fig. 2, *lane 8*) (35). A less prominent band of ~40 kDa could be immunoprecipitated with antiserum to SecY (Fig. 2, *lane 9*) (35).

In summary, using this unbiased approach it was shown that, at a nascent chain length of 88 amino acids, TM1 of MalF interacts with TF, SRP, and L23 and inserts into the inner membrane in a carbonate-resistant state close to YidC and SecY. This strongly suggests that MalF is targeted via the SRP pathway to the SecY/YidC insertion site in the inner membrane.

TM1 of MalF Remains Close to YidC and the Sec Translocon during Insertion of TM2 and TM3 of MalF into the Membrane, and TM2 and TM3 Insert into the Membrane in a Molecular Environment Similar to That of TM1—To study the sequence of events taking place during the biogenesis of the three N-terminal TMs of MalF, nascent chains of increasing lengths were synthesized *in vitro*. The shortest nascent chain, 68MalF, is expected to fully expose the first TM segment from the ribosome nascent chain complex (see Fig. 3*A*). At a length of 100 amino acids, 100MalF exposes TM1 and TM2. 131MalF, the longest nascent chain, exposes TM1, TM2, and TM3. By placing a TAG codon at position 26 and by exploiting the photo-cross-linking procedure described above, the molecular environment of TM1 in each of these translation intermediates was studied. C-terminal c-Myc epitope tags were introduced to enable purification of nascent chains by immunoprecipitation. Previous work has shown that this approach can prevent misinterpretations of cross-linking experiments due to premature termination of translation (41).

For each of the constructs, the TAG codon was suppressed, and nascent MalF of the expected apparent molecular weight was produced (data not shown). As shown in Fig. 3*B*, all nascent chains could be immunoprecipitated using the anti-c-Myc antibodies. Upon UV irradiation, several adducts were resolved and co-immunoprecipitated with the nascent chains of desired length. 68MalFTAG26-Myc cross-linked YidC and SecY (Fig. 3*B*, *lane 1*). Also, an adduct of ~25 kDa was present that could be precipitated with anti-SecE (Fig. 3*C*, *lane 3*). As expected, the 100MalFTAG26-Myc nascent chain was cross-linked to YidC and SecY, similar to 88MalFTAG26 (compare Fig. 2, *lane 7* to Fig. 3*B*, *lane 2*), because both constructs expose TM1 and TM2 and share a cross-link site at an identical position. Notably, the SecE cross-link was lost at this length. These cross-links represent the molecular environment of TM1 after both TM1 and TM2 are completely exposed outside the ribosome (Fig. 3*A*). Upon further extension of the MalF nascent chain to a length of 131 amino acids, the photoprobe in TM1 continued to cross-link YidC and SecY, whereas the SecE adduct reappeared (Fig. 3*B*, *lane 4*). These results show that TM1 of MalF initially

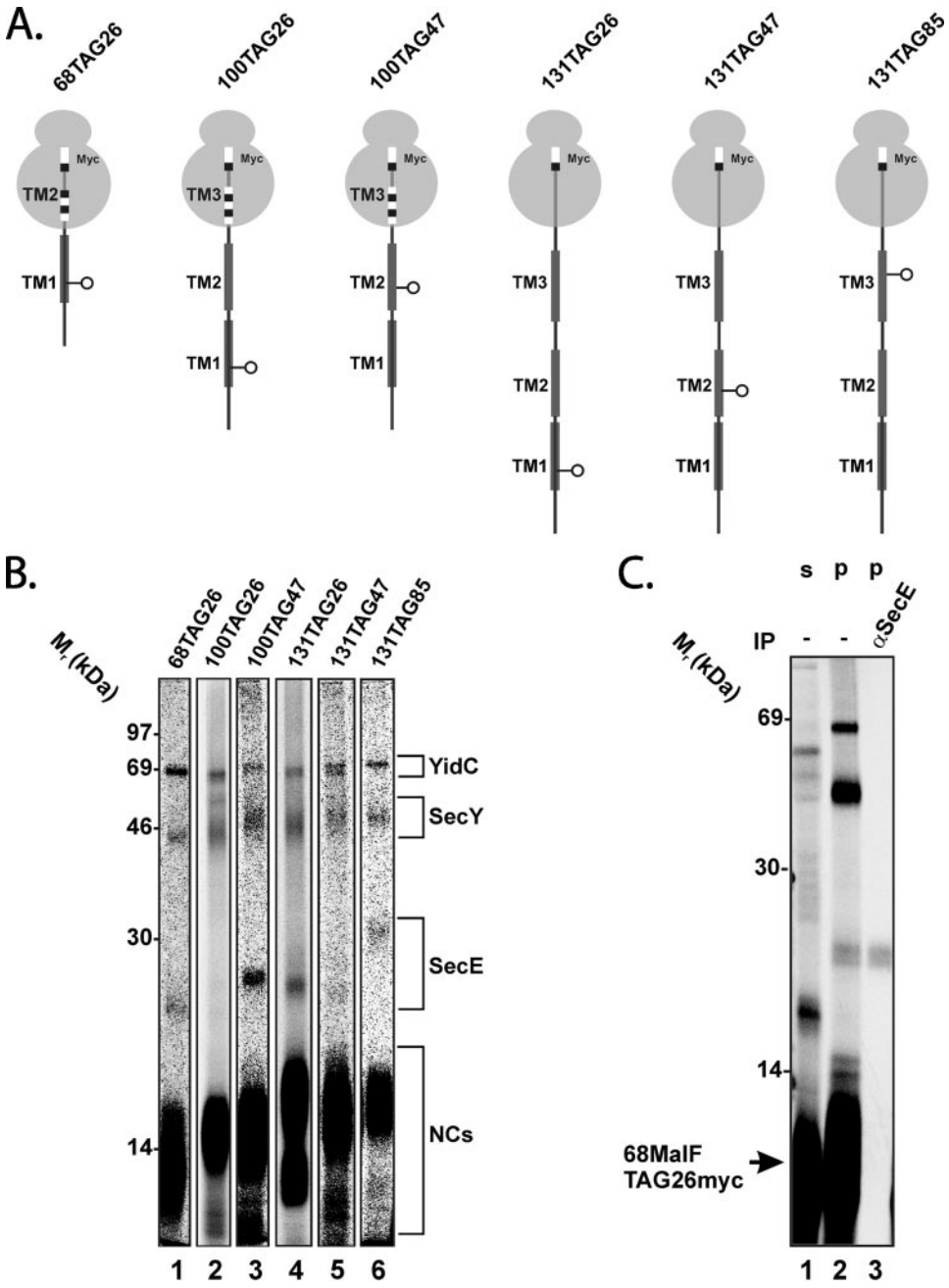

FIGURE 3. **The molecular environment of MalF TM1, -2, and -3.** *A*, schematic representation of MalF ribosome nascent chain complexes. TMs exposed outside the ribosome are *dark gray*, and TMs buried inside the ribosomal tunnel are *black* and *white*. The *open circle* indicates the position of the cross-linking site. All nascent chains contain a C-terminal Myc tag (*Myc*). *B*, MalF mRNAs containing single UAG codons were used to synthesize the corresponding nascent chains in the presence of (Tmd)Phe-tRNA^{Sup} and *E. coli* wild-type IMVs *in vitro*. After translation, samples were cross-linked by UV irradiation. The pellet fraction of a carbonate extraction was subjected to immunoprecipitation with anti-Myc antibodies. Immunoprecipitated samples were subjected to SDS-PAGE and phosphorimaging. The positions in the gel of nascent chains (*NCs*), and cross-links to YidC, SecY, and SecE are indicated. *C*, 68MalFTAG26 was synthesized and UV-cross-linked as described in *B*. Carbonate extraction was used to separate membrane integrated (*p*) from soluble and peripheral membrane proteins (*s*). Anti-SecE antibodies were used for immunoprecipitation. Samples were further processed as described in *B*.

inserts into the membrane in a carbonate resistant form close to YidC, SecY, and SecE. At all nascent chain lengths studied here, the contacts of TM1 with YidC and SecY remain. The SecE contact is temporarily lost upon extension of the nascent chain, but reappears at a later stage, when TM1, TM2, and TM3 have all left the confinement of the ribosome.

The interactions of TM2 were mapped by establishing the cross-links of 100MalFTAG47-Myc and 131MalFTAG47-Myc nascent chains. With both constructs, cross-links to YidC, SecY, and SecE were co-immunoprecipitated with the nascent chains by anti-C-Myc antibody (Fig. 3*B*, *lanes 3* and *5*). 131MalFTAG85-Myc was also cross-linked to YidC, SecY, and SecE, indicating that the molecular environment of TM3 at this stage of biogenesis was comparable to that of TM1 and TM2 (Fig. 3*B*, *lane 6*). These data indicate that TM2 and TM3 initially insert into the membrane close to YidC, SecY, and SecE and therefore behave like TM1. TM2 also remains close to these proteins when TM3 has inserted into the membrane. This indicates that at least the first three TMs of MalF assemble simultaneously at the Sec/YidC insertion site in the inner membrane and do not partition completely into the lipids at this stage in biogenesis.

Efficient Membrane Targeting and Insertion of MalF Requires SRP and the Sec Translocon—Next, targeting and insertion of full-length MalF expressed from a plasmid were monitored *in vivo* in SRP and Sec translocon mutant strains by analyzing the proteinase K accessibility of MalF in spheroplasts. OmpA, outer membrane protein A, served as a positive control for spheroplast formation by monitoring the proteinase K sensitivity of its periplasmic domain (42). Band X, a cytoplasmic protein, is a negative control. It is used to confirm the spheroplasts are intact (42).

Depletion of the essential SRP component 4.5 S RNA compromises the SRP-targeting pathway (43). Depletion of 4.5 S RNA strongly inhibited proteolysis of MalF in spheroplasts, as compared with spheroplasts made of non-depleted (control) cells (Fig. 4*A*). Notably, processing of the Sec-dependent OmpA protein was not affected upon 4.5 S RNA depletion, which shows that the Sec translocon was functional under these conditions. Assembly of MalF was further studied in a SecE depletion strain. Upon depletion of SecE, SecY is rapidly degraded by the FtsH protease resulting in the loss of the

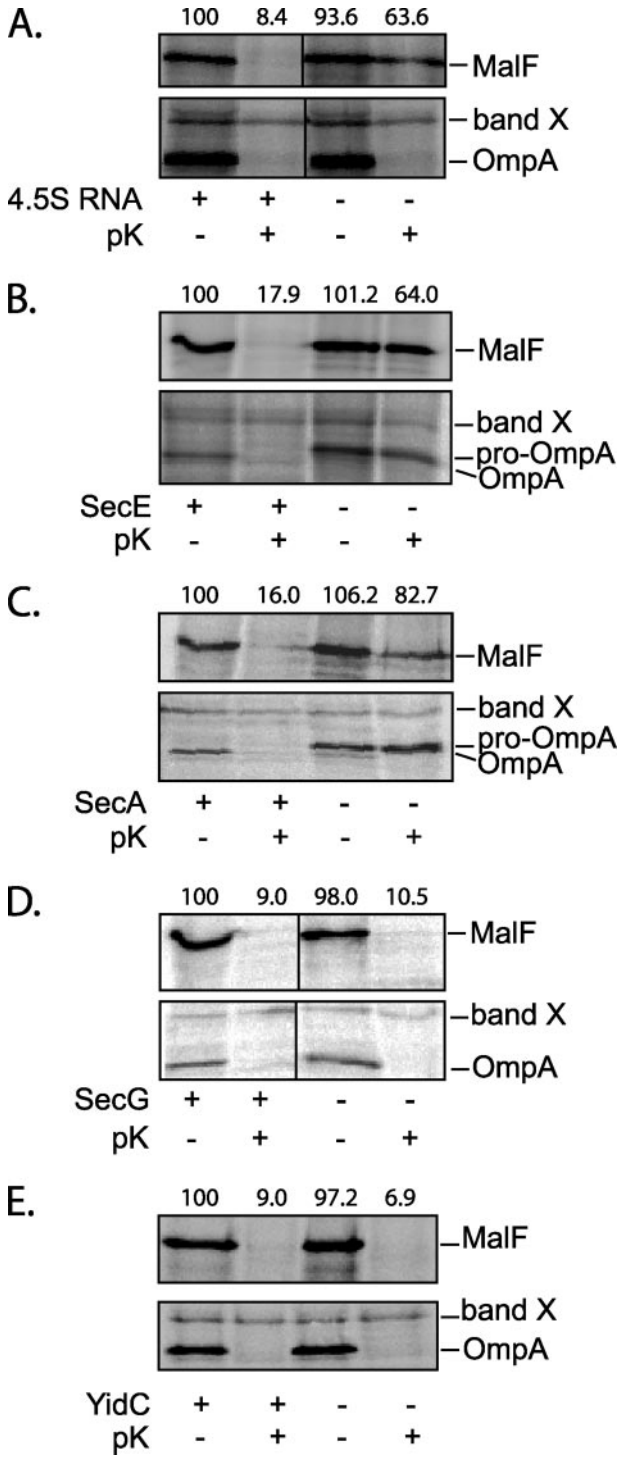

FIGURE 4. **Membrane insertion of MalF is SRP/SecAYE-dependent and YidC-independent.** *A*, proteinase K accessibility of MalF (*top*) and OmpA/bandX (*bottom*) in FF283 (4.5 S RNA depletion strain) spheroplasts, made from cells cultured in the presence/absence of IPTG (+, non-depleted cells; −, depleted cells). Cells were pulse-labeled and processed as described under "Experimental Procedures." OmpA is only degraded by proteinase K in cells with a disrupted outer membrane. OmpA secretion/processing was not affected upon SRP-depletion. *band X* is a cytoplasmic control and is not degraded by proteinase K in spheroplasts. *B*, proteinase K accessibility of MalF (*top*) and OmpA/bandX (*bottom*) in CM124 (SecE depletion strain) spheroplasts, made from cells cultured in the presence/absence of arabinose (+, non-depleted cells; −, depleted cells). Cells were pulse-labeled and processed as described under "Experimental Procedures." OmpA secretion/processing is affected upon SecE-depletion. *C*, proteinase K accessibility of MalF (*top*) and OmpA/bandX (*bottom*) in BA13 and DO251 (SecA depletion strain and control) spheroplasts, made from cells cultured at 41 °C (+, non-depleted cells; −, depleted cells). Cells were pulse-labeled and processed as described under "Experimental Procedures." OmpA secretion/processing is affected upon SecA-depletion. *D*, proteinase K accessibility of MalF (*top*) and OmpA/bandX (*bottom*) in KN370/KN370 harboring pH^+ (SecG deletion strain, pH^+ plasmid expressing SecG) spheroplasts. Cells were pulse-labeled and processed as described under "Experimental Procedures." OmpA secretion/processing was not affected in the absence of SecG. *E*, proteinase K accessibility of MalF (*top*) and OmpA/bandX (*bottom*) in FTL10 (YidC depletion strain) spheroplasts, made from cells cultured in the presence/absence of arabinose (+, non-depleted cells; −, depleted cells). Cells were pulse-labeled and processed as described under "Experimental Procedures." OmpA secretion/processing was not affected upon YidC depletion. MalF bands were quantified, and the band volumes of spheroplasts made of control cells not treated with proteinase K were set to 100%.

SecY/E core of the translocon (44). Depletion of SecE strongly inhibited proteolysis of MalF in spheroplasts, as compared with non-depleted (control) cells (Fig. 4*B* and Ref. 45). As expected, processing and translocation of the Sec-dependent OmpA was strongly affected upon SecE depletion. Upon depletion of SecA, which does not affect the rest of the Sec translocon (46), proteolysis of MalF in spheroplasts was strongly reduced compared with the control sample (Fig. 4*C*). This indicates that SecA is required for the biogenesis, presumably by energizing the translocation of the periplasmic loop between TM3 and -4. Processing and translocation of OmpA were, as expected, also affected upon SecA depletion. Finally, the insertion of MalF was not affected in the absence of the non-essential Sec translocon component SecG (Fig. 4*D*).

Taken together, these data indicate that MalF is targeted to the inner membrane via the SRP pathway and that insertion of MalF into the inner membrane is SecAYE-dependent. This is in keeping with the *in vitro* cross-linking data described above and previous *in vivo* studies (*e.g.* Refs. 45, 47, 48).

Insertion of MalF into the Inner Membrane Does Not Depend on YidC—The close proximity of nascent MalF to YidC during insertion in the membrane as shown by cross-linking (see Figs. 2 and 3) suggests that YidC plays an important role in the biogenesis of MalF. Therefore, insertion of plasmid-expressed MalF into the inner membrane was monitored in the YidC depletion strain FTL10 by analyzing the proteinase K accessibility of MalF in spheroplasts (Fig. 4*E*). Insertion of MalF into the inner membrane was not affected upon the depletion of YidC. Cells were efficiently depleted of YidC as determined by immunoblotting (data not shown), and the translocation of OmpA was, as expected, not affected upon YidC depletion.

To study the role of YidC in the insertion of MalF into the inner membrane *in vivo* in more detail, we used a very sensitive biotinylation assay (28). Two MalF derivatives were engineered, one containing the *Propionibacterium shermanii* transcarboxylase (PSBT) biotin-accepting domain from the 1.3 S subunit of PSBT in the large periplasmic loop between TM3 and -4 (MalF-PBST I), and the other containing the PBST domain in the small cytoplasmic loop between TM4 and -5 (MalF-PBST L) (Fig. 1). The PSBT domain is biotinylated by the cytoplasmic enzyme biotin ligase. Hence, to be biotinylated, the PBST domain must at least temporarily be exposed to the cytoplasm (28). As expected, MalF-PSBT L was efficiently biotinylated irrespective of the presence/depletion of YidC (Fig. 5). MalF-PSBT I was neither in the presence nor upon the depletion of YidC biotin-

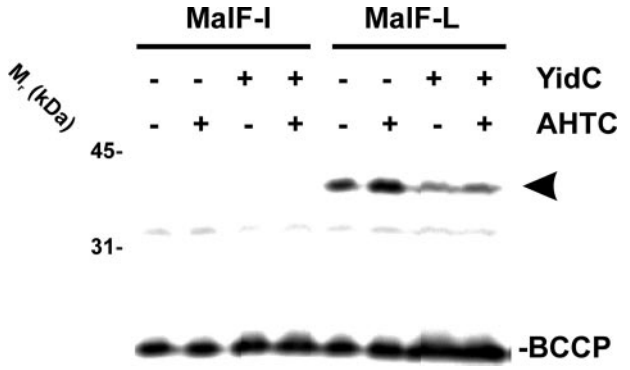

FIGURE 5. **MalF-PBST I and MalF-PBST L (see Fig. 1) were expressed in FTL10*malF*::*Tn10* (pASK-IBA*lacI*) grown either in the presence (YidC+) or absence (YidC−) of arabinose.** Anhydrotetracycline was either added to a final concentration of 0.2 μg/ml or excluded from the medium. Samples were collected and processed for SDS-PAGE and Western blotting as described under "Experimental Procedures." Streptavidin-horseradish peroxidase conjugate was used for detection of biotinylated proteins. The *arrowhead* indicates the position of MalF-PBST L on gel. Biotin carboxyl carrier protein (*BCCP*) was detected in all samples and was used as a loading control.

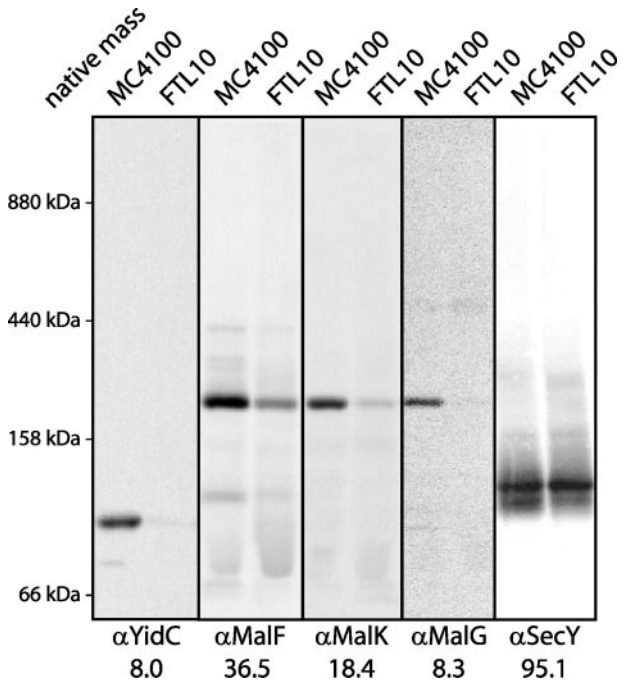

FIGURE 6. **Reduced accumulation levels of the MalFGK$_2$ maltose transport complex upon YidC depletion.** MC4100*ara*$^+$ and FTL10 cells were cultured in LB medium in the presence of maltose. Complexes in purified inner membranes were separated by blue native-PAGE, and proteins were subsequently transferred to a polyvinylidene difluoride membrane. Blots were decorated with antibodies to YidC, SecY, and the maltose transport complex components MalF, -K, and -G. MalFGK$_2$, YidC, and SecYEG bands were quantified, and the band volumes of purified membranes of control cells were set to 100%. The *numbers* represent the intensities upon YidC depletion.

ylated (Fig. 5). This indicates that translocation of the periplasmic loop between TM3 and -4 proceeds normally in the absence of YidC in a co-translational mechanism. To verify that the cells were efficiently depleted of YidC, the samples were also subjected to immunoblotting using YidC-specific antibodies (data not shown). Furthermore, to confirm that MalF-PSBT-I and -L were synthesized at comparable levels, the blots were also decorated with MalF antiserum (data not shown). Taken together, these experiments suggest that YidC is not required for the insertion of MalF into the inner membrane.

YidC Depletion Leads to Reduced Accumulation Levels of the MalFGK$_2$ Maltose Transport Complex—Although the insertion of MalF in the inner membrane is YidC-independent, the close proximity of different regions of nascent MalF to YidC during insertion points to an important role of YidC in the biogenesis of MalF. Therefore, as a next step in the characterization of the role of YidC in the biogenesis of MalF, the accumulation levels of endogenously expressed MalFGK$_2$ maltose transport complex in inner membranes isolated from cells depleted of YidC and control cells were monitored. To this end, membrane complexes were separated by blue native-PAGE, and proteins were subsequently transferred to a polyvinylidene difluoride membrane. Membranes were decorated with antibodies to the maltose transport complex components MalF, -K, and -G and to the translocon components YidC and SecY (Fig. 6). Strikingly, accumulation of the maltose transport complex was strongly reduced upon YidC depletion (~80% down). In contrast, complex formation of the SecYEG-hetrotrimer was hardly affected (~5% down). This shows that YidC is involved in the biogenesis of the maltose transport complex, that this effect is not general, and that the reduced maltose transport complex levels are not due to reduced Sec translocon levels.

YidC Is Required for the Stability of MalF—Subsequently, the steady-state level of endogenously expressed MalF in the inner membrane of cells depleted of YidC and control cells was monitored by immunoblotting. Upon YidC depletion, the accumulation level of full-length MalF was strongly reduced, and two putative MalF degradation products appeared (Fig. 7*A*). YidC depletion did not affect the level of MalG, whereas the level of MalK attached to the membrane and in whole cells was affected (~70% down) upon YidC depletion (Fig. 7*A*).

The immunoblotting experiments could mean that YidC is required for the stability of MalF. To monitor the stability of MalF upon YidC depletion in more detail, a pulse-chase approach was used. Cells depleted of YidC and control cells were cultured and labeled with [^{35}S]methionine as described under "Experimental Procedures." After chases of 3, 30, and 60 min, MalF was isolated by means of immunoprecipitation, and precipitated material was subsequently analyzed by SDS-PAGE and phosphorimaging (Fig. 7*B*). After a chase of 3 min, the amount of MalF was similar in cells expressing and depleted of YidC. However, in cells depleted of YidC the MalF signal strongly decreased in time, whereas it remained stable in the control cells. Because the level of MalK in cells depleted of YidC was lower than in wild-type cells, MalF stability was also monitored in cells not expressing its complex partners MalK and MalG (Fig. 7*B*). In both *malK* and *malG* deletion strains MalF stability was not affected, which is in keeping with observations made by Traxler and Beckwith (22). This indicates that YidC is important for MalF stability rather than its complex partners MalF and MalG.

DISCUSSION

So far, the role of YidC in the folding of complex membrane proteins has only been studied in detail for the monomeric membrane protein lactose permease (LacY). It was shown,

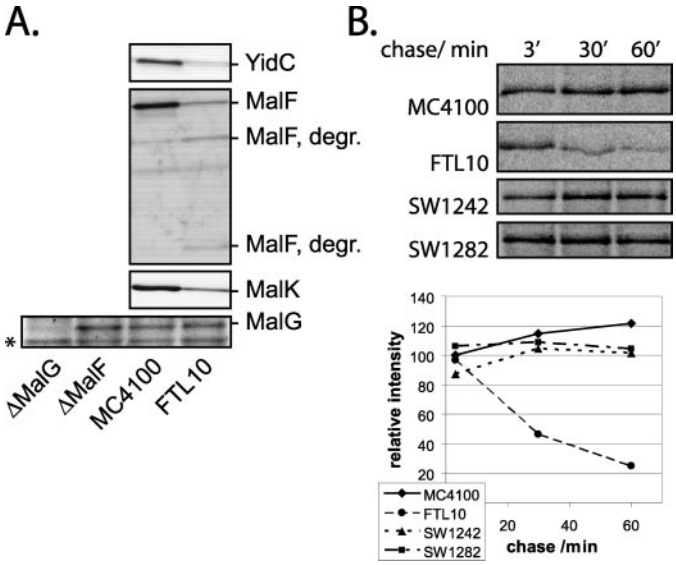

FIGURE 7. **YidC is required for the stability of MalF.** *A*, MC4100*ara*$^+$ and FTL10 cells were cultured in LB medium in the presence of maltose. Inner membranes were isolated and analyzed by SDS-PAGE and immunoblotting with antibodies directed against YidC, MalK, -F, and -G. The band in the αMalG blot that is marked with an *asterisk* is a background band, which indicates that equal amounts of membranes were loaded. *B*, MC4100*ara*$^+$, FTL10, SW1242(Δ*malG*), and SW1282(Δ*malK*) cells were cultured in LB medium in the presence of maltose and labeled with [^{35}S]methionine as described under "Experimental Procedures." 3, 30, and 60 min after an excess of cold methionine was added to the cultures, cells were precipitated with trichloroacetic acid, and MalF was subsequently isolated by immunoprecipitation. Immunoprecipitations were analyzed by SDS-PAGE and phosphorimaging (*upper panel*). Relative band volumes are shown in the graph in the *lower panel*.

using *in vitro* reconstitution approaches and a folding assay based on monoclonal antibodies against conformational epitopes of LacY, that YidC is required for the co-translational folding of LacY (16). As a consequence, the stability of LacY was affected upon YidC depletion (16). Here, we have studied the role of YidC in the folding of a polytopic inner membrane protein that is part of a hetero-oligomeric complex. Using a combination of an *in vitro* cross-linking approach, *in vivo* biogenesis assays, and blue native-PAGE we have monitored the role of YidC at different stages in the biogenesis of MalF, which is a constituent of the MalFGK$_2$ maltose transport complex. First however, we re-evaluated the SRP/Sec dependence of MalF, because not all studies on its SRP/Sec dependence were conclusive.

Targeting of MalF via the SRP pathway had been studied before using genetic approaches. In the Slo (synthetic lethality upon overexpression) screen, which was developed by Bernstein and co-workers (49), MalF was not identified as an SRP substrate. Furthermore, blocking of the SRP-targeting pathway by overexpression of a non-functional variant of the SRP-receptor FtsY only marginally affected the insertion of a MalF alkaline phosphatase fusion protein (49). However, in a genetic screen designed to isolate *E. coli* mutants affected in membrane protein assembly, a strain with a mutation in the *ffs* gene, which encodes the SRP component 4.5 S RNA, was isolated that affected the targeting of a MalF LacZ fusion protein (47). In the present study we show that Ffh, a component of the SRP, can be readily cross-linked to TM1 of nascent MalF *in vitro* and that the *in vivo* targeting of full-length MalF is strongly hampered in cells depleted of the SRP component 4.5 S RNA. It should be mentioned that the observed cross-linking to Ffh is highly significant considering the extremely low abundance of Ffh in wild-type cells and hence in the translation lysate used in this assay (50). This strongly suggests that, at least a considerable fraction of, MalF is targeted to the inner membrane via the SRP pathway. In short MalF nascent chains, TM1 not only interacts with Ffh, but also with the ribosomal protein L23, which is located near the exit of the ribosomal tunnel, and the chaperone TF (37). SRP and the chaperone TF bind simultaneously to L23 (51, 52). TF generically binds nascent peptides exiting the ribosome (53). Neither TF depletion nor overproduction has any notable effect on MalF membrane targeting/insertion.[6] This is in keeping with the notions that TF and SRP sample nascent chains on the ribosome in a nonexclusive fashion, and that binding of the SRP receptor, FtsY, to ribosome-bound SRP excludes TF from the ribosome allowing the docking of the ribosome to the Sec translocon (51).

Most SRP-dependent proteins studied thus far are targeted to the Sec translocon in the inner membrane (1, 3). Indeed, by means of *in vitro* cross-linking using MalF nascent chains of different length, we showed that the first three TMs of MalF insert and remain in the vicinity of the Sec translocon core components SecY and SecE during the biogenesis of MalF. Consistently, *in vivo* assembly of MalF is affected upon SecE depletion (our data and Ref. 45). This is also in keeping with the observation that the membrane insertion of a MalF alkaline phosphatase fusion is affected in a strain with a mutation in SecY that specifically affects the biogenesis of inner membrane proteins (45, 54). In a SecG null mutant background there was no effect on the insertion of MalF into the membrane.

Thus far, azide, an inhibitor of SecA, has been used to show that SecA is involved in the biogenesis of MalF (45). To examine the involvement of SecA in the biogenesis of MalF more directly, we monitored the assembly of MalF in a SecA depletion strain. Upon depletion of SecA, which does not affect the rest of the Sec translocon (46), insertion of MalF into the inner membrane was strongly hampered. Taken together, biogenesis of MalF appears to be SRP/SecAYE-dependent.

Using two different assays, it was shown here that *in vivo* insertion and topogenesis of MalF into the membrane were not affected upon YidC depletion. However, *in vitro* cross-linking experiments demonstrated that the first three TMs of MalF not only insert into the membrane close to SecY and SecE but also to YidC. Notably, they remain in this environment at least until the first three TMs of MalF have emerged from the ribosome in the co-translational insertion process. Correspondingly, it has been shown that the first TMs of the nascent polytopic inner membrane protein MtlA assemble simultaneously at the Sec/YidC insertion site (15). Recently, docking of the projection maps of YidC and the SecYEG translocon generated a potential contiguous pathway for translocating TMs (55). This pathway could provide an environment for the TMs where their folding and assembly can occur prior to their release into the lipid bilayer. The integration of aquaporin-4 into the endoplasmic

[6] S. Wagner, O. Pop, G.-J. Haan, L. Baars, G. Koningstein, M. M. Klepsch, P. Genevaux, J. Luirink, and J.-W. de Gier, unpublished results.

reticulum membrane by the Sec61 translocon has been shown to involve sequential triage of TMs from their initial portal of entry into multiple secondary sites within the translocon (56). It was proposed that this mechanism provided a means to facilitate early folding events before release into the lipid bilayer. It has been speculated that the endoplasmic reticulum-localized TRAM protein has a similar function as YidC, and it has also been shown that there are specialized chaperones in the endoplasmic reticulum mediating the co-translational folding of specific membrane proteins (57–59).

In contrast to the TMs of MalF, MtlA, and aquaporin-4, the two TMs of the inner membrane protein leader peptidase (Lep) partition one by one into the lipid bilayer via the Sec/YidC interface according to the linear insertion model of TMs (41). A possible explanation for this discrepancy may relate to the role of the TMs in the respective proteins. The TMs of Lep merely act as a membrane anchor for the periplasmic P2 domain of Lep to which the catalytic activity of Lep is confined, whereas the TMs of MtlA, MalF, and aquaporin-4 play key roles in the functioning of these proteins. Proper folding and interaction of the TMs of MalF, MtlA, and aquaporin-4 is an absolute requirement for the functioning of these proteins and may also be a prerequisite for complex formation.

The cross-linking data are consistent with the notion that YidC functions in co-translational folding of complex inner membrane proteins. The importance of YidC in membrane protein folding and assembly is also suggested by the observation that YidC depletion leads to the induction of Cpx and σ^E envelope stress responses that sense protein abnormalities in the inner and outer membranes as well as in the periplasm (17, 18). Misfolding or misassembly of membrane proteins is often linked to decreased stability (60). Although MalF was rapidly degraded upon YidC depletion, the absence of the other constituents of the MalFGK$_2$ complex did not affect the stability of the protein as judged by pulse-chase analysis. However, trypsin accessibility experiments showed that the folding of the large periplasmic loop of MalF is not completed before it is incorporated into the MalFGK$_2$ complex (22).[6] Possibly, YidC mainly chaperones the initial folding of MalF by acting on its integral membrane part, which is likely to be critical for MalF stability and hence for assembly of MalFGK$_2$ complexes.

In the *mal* operon, the gene encoding MalG is located downstream of the gene encoding MalF; *i.e.* MalG is synthesized after MalF and most likely will insert after MalF into the membrane. It is tempting to speculate that MalF is kept by YidC in a conformation that allows a smooth MalF-MalG complex formation. However, we did not manage to isolate Sec/YidC-MalF complexes (results not shown). In contrast, the YidC homolog in the thylakoidal membrane, Albino3, could be isolated in a complex within the membrane-inserted D1 protein, before it was incorporated into the photosystem II complex (61). The Sec and/or YidC-MalF complexes, if they indeed exist, may be too fragile or transient to purify.

Summarizing, we have shown that the polytopic integral membrane protein MalF, which is a constituent of the MalFGK$_2$ complex, is targeted to the inner membrane via the SRP pathway to the Sec/YidC insertion site. Despite close proximity of nascent MalF to YidC during insertion, YidC is not required for the insertion of MalF into the membrane. However, YidC is required for the stability of MalF and the formation of the MalFGK$_2$ maltose transport complex. Our data indicate that YidC supports the folding of MalF into a stable conformation before it is incorporated into the maltose transport complex.

Acknowledgments—We thank Jon Beckwith, Richard Brimacombe, Amy Davidson, Frank Sargent, and Josef Brunner for strains, sera, and reagents. We thank W. S. P. Jong for useful comments during preparation of the manuscript. Research in the laboratory of J. W. de Gier is supported by the Swedish Research Council, the Swedish Foundation for Strategic Research, and the Marcus and Marianne Wallenberg Foundation.

REFERENCES

1. Luirink, J., von Heijne, G., Houben, E., and de Gier, J. W. (2005) *Annu. Rev. Microbiol.* **59,** 329–355
2. Luirink, J., and Sinning, I. (2004) *Biochim. Biophys. Acta* **1694,** 17–35
3. Facey, S. J., and Kuhn, A. (2004) *Biochim. Biophys. Acta* **1694,** 55–66
4. Van den Berg, B., Clemons, W. M., Jr., Collinson, I., Modis, Y., Hartmann, E., Harrison, S. C., and Rapoport, T. A. (2004) *Nature* **427,** 36–44
5. Veenendaal, A. K., van der Does, C., and Driessen, A. J. (2004) *Biochim. Biophys. Acta* **1694,** 81–95
6. Rapoport, T. A. (2007) *Nature* **450,** 663–669
7. Osborne, A. R., Rapoport, T. A., and van den Berg, B. (2005) *Annu. Rev. Cell Dev. Biol.* **21,** 529–550
8. Clemons, W. M., Jr., Menetret, J. F., Akey, C. W., and Rapoport, T. A. (2004) *Curr. Opin. Struct. Biol.* **14,** 390–396
9. Dalbey, R. E., and Chen, M. (2004) *Biochim. Biophys. Acta* **1694,** 37–53
10. Kiefer, D., and Kuhn, A. (2007) *Int. Rev. Cytol.* **259,** 113–138
11. Xie, K., and Dalbey, R. E. (2008) *Nat. Rev. Microbiol.* **6,** 234–244
12. Houben, E. N., Scotti, P. A., Valent, Q. A., Brunner, J., de Gier, J. L., Oudega, B., and Luirink, J. (2000) *FEBS Lett.* **476,** 229–233
13. Urbanus, M. L., Scotti, P. A., Froderberg, L., Saaf, A., de Gier, J. W., Brunner, J., Samuelson, J. C., Dalbey, R. E., Oudega, B., and Luirink, J. (2001) *EMBO Rep.* **2,** 524–529
14. Scotti, P. A., Urbanus, M. L., Brunner, J., de Gier, J. W., von Heijne, G., van der Does, C., Driessen, A. J., Oudega, B., and Luirink, J. (2000) *EMBO J.* **19,** 542–549
15. Beck, K., Eisner, G., Trescher, D., Dalbey, R. E., Brunner, J., and Müller, M. (2001) *EMBO Rep.* **2,** 709–714
16. Nagamori, S., Smirnova, I. N., and Kaback, H. R. (2004) *J. Cell Biol.* **165,** 53–62
17. Shimohata, N., Chiba, S., Saikawa, N., Ito, K., and Akiyama, Y. (2002) *Genes Cells* **7,** 653–662
18. Shimohata, N., Nagamori, S., Akiyama, Y., Kaback, H. R., and Ito, K. (2007) *J. Cell Biol.* **176,** 307–317
19. Ehrmann, M., Ehrle, R., Hofmann, E., Boos, W., and Schlosser, A. (1998) *Mol. Microbiol.* **29,** 685–694
20. Oldham, M. L., Khare, D., Quiocho, F. A., Davidson, A. L., and Chen, J. (2007) *Nature* **450,** 515–521
21. Froshauer, S., Green, G. N., Boyd, D., McGovern, K., and Beckwith, J. (1988) *J. Mol. Biol.* **200,** 501–511
22. Traxler, B., and Beckwith, J. (1992) *Proc. Natl. Acad. Sci. U. S. A.* **89,** 10852–10856
23. Mourez, M., Hofnung, M., and Dassa, E. (1997) *EMBO J.* **16,** 3066–3077
24. Froderberg, L., Houben, E., Samuelson, J. C., Chen, M. Y., Park, S. K., Phillips, G. J., Dalbey, R., Luirink, J., and de Gier, J. W. L. (2003) *Mol. Microbiol.* **47,** 1015–1027
25. Hatzixanthis, K., Palmer, T., and Sargent, F. (2003) *Mol. Microbiol.* **49,** 1377–1390
26. Guzman, L. M., Belin, D., Carson, M. J., and Beckwith, J. (1995) *J. Bacteriol.* **177,** 4121–4130
27. Hashemzadeh-Bonehi, L., Mehraein-Ghomi, F., Mitsopoulos, C., Jacob,

J. P., Hennessey, E. S., and Broome-Smith, J. K. (1998) *Mol. Microbiol.* **30,** 676–678
28. Jander, G., Cronan, J. E., and Beckwith, J. (1996) *J. Bacteriol.* **178,** 3049–3058
29. Wagner, S., Baars, L., Ytterberg, A. J., Klussmeier, A., Wagner, C. S., Nord, O., Nygren, P. A., van Wijk, K. J., and de Gier, J. W. (2007) *Mol. Cell Proteomics* **6,** 1527–1550
30. Schagger, H., and von Jagow, G. (1991) *Anal. Biochem.* **199,** 223–231
31. Datsenko, K. A., and Wanner, B. L. (2000) *Proc. Natl. Acad. Sci. U. S. A.* **97,** 6640–6645
32. Miller, J. H. (1992) *A Short Course in Bacterial Genetics*, Cold Spring Harbor Laboratory Press, Cold Spring Harbor, NY
33. Houben, E. N., Zarivach, R., Oudega, B., and Luirink, J. (2005) *J. Cell Biol.* **170,** 27–35
34. Ullers, R. S., Houben, E. N., Raine, A., ten Hagen-Jongman, C. M., Ehrenberg, M., Brunner, J., Oudega, B., Harms, N., and Luirink, J. (2003) *J. Cell Biol.* **161,** 679–684
35. de Gier, J. W., and Luirink, J. (2003) *EMBO Rep.* **4,** 939–943
36. Ferbitz, L., Maier, T., Patzelt, H., Bukau, B., Deuerling, E., and Ban, N. (2004) *Nature* **431,** 590–596
37. Ban, N., Nissen, P., Hansen, J., Moore, P. B., and Steitz, T. A. (2000) *Science* **289,** 905–920
38. Gu, S. Q., Peske, F., Wieden, H. J., Rodnina, M. V., and Wintermeyer, W. (2003) *RNA* (*N. Y.*) **9,** 566–573
39. Kramer, G., Rauch, T., Rist, W., Vorderwulbecke, S., Patzelt, H., Schulze-Specking, A., Ban, N., Deuerling, E., and Bukau, B. (2002) *Nature* **419,** 171–174
40. Halic, M., Gartmann, M., Schlenker, O., Mielke, T., Pool, M. R., Sinning, I., and Beckmann, R. (2006) *Science* **312,** 745–747
41. Houben, E. N., ten Hagen-Jongman, C. M., Brunner, J., Oudega, B., and Luirink, J. (2004) *EMBO Rep.* **5,** 970–975
42. de Gier, J.-W. L., Mansournia, P., Valent, Q., Phillips, G. J., Luirink, J., and von Heijne, G. (1996) *FEBS Lett.* **399,** 307–309
43. Ribes, V., Romisch, K., Giner, A., Dobberstein, B., and Tollervey, D. (1990) *Cell* **63,** 591–600
44. Akiyama, Y., Kihara, A., Tokuda, H., and Ito, K. (1996) *J. Biol. Chem.* **271,** 31196–31201
45. Traxler, B., and Murphy, C. (1996) *J. Biol. Chem.* **271,** 12394–12400
46. Qi, H. Y., and Bernstein, H. D. (1999) *J. Biol. Chem.* **274,** 8993–8997
47. Tian, H., Boyd, D., and Beckwith, J. (2000) *Proc. Natl. Acad. Sci. U. S. A.* **97,** 4730–4735
48. Tian, H., and Beckwith, J. (2002) *J. Bacteriol.* **184,** 111–118
49. Ulbrandt, N. D., Newitt, J. A., and Bernstein, H. D. (1997) *Cell* **88,** 187–196
50. Adams, H., Scotti, P. A., de Cock, H., Luirink, J., and Tommassen, J. (2002) *Eur. J. Biochem.* **269,** 5564–5571
51. Buskiewicz, I., Deuerling, E., Gu, S. Q., Jockel, J., Rodnina, M. V., Bukau, B., and Wintermeyer, W. (2004) *Proc. Natl. Acad. Sci. U. S. A.* **101,** 7902–7906
52. Raine, A., Ivanova, N., Wikberg, J. E., and Ehrenberg, M. (2004) *Biochimie* (*Paris*) **86,** 495–500
53. Patzelt, H., Rudiger, S., Brehmer, D., Kramer, G., Vorderwulbecke, S., Schaffitzel, E., Waitz, A., Hesterkamp, T., Dong, L., Schneider-Mergener, J., Bukau, B., and Deuerling, E. (2001) *Proc. Natl. Acad. Sci. U. S. A.* **98,** 14244–14249
54. Newitt, J. A., and Bernstein, H. D. (1998) *J. Biol. Chem.* **273,** 12451–12456
55. Lotz, M., Haase, W., Kuhlbrandt, W., and Collinson, I. (2008) *J. Mol. Biol.* **375,** 901–907
56. Sadlish, H., Pitonzo, D., Johnson, A. E., and Skach, W. R. (2005) *Nat. Struct. Mol. Biol.* **12,** 870–878
57. Johnson, A. E., and van Waes, M. A. (1999) *Annu. Rev. Cell Dev. Biol.* **15,** 799–842
58. Kota, J., and Ljungdahl, P. O. (2005) *J. Cell Biol.* **168,** 79–88
59. Kota, J., Gilstring, C. F., and Ljungdahl, P. O. (2007) *J. Cell Biol.* **176,** 617–628
60. Ito, K., and Akiyama, Y. (2005) *Annu. Rev. Microbiol.* **59,** 211–231
61. Ossenbuhl, F., Gohre, V., Meurer, J., Krieger-Liszkay, A., Rochaix, J. D., and Eichacker, L. A. (2004) *Plant Cell* **16,** 1790–1800

ADDITIONS AND CORRECTIONS

This paper is available online at www.jbc.org

THE JOURNAL OF BIOLOGICAL CHEMISTRY VOL. 284, NO. 52, p. 36720, December 25, 2009

VOLUME 284 (2009) PAGES 30547–30555
DOI 10.1074/jbc.A109.040964

Dual activities of odorants on olfactory and nuclear hormone receptors.

Horst Pick, Sylvain Etter, Olivia Baud, Ralf Schmauder, Lorenza Bordoli, Torsten Schwede, and Horst Vogel

On page 30551, Table 1, first column, the experimentally determined values of EC_{50} of ER activation for MC, Polysantol, Javanol, and androstenol have been presented with the wrong concentration (mM). The correct concentration is μM.

TABLE 1

Estrogenic activities of odorants

The compound concentrations (EC_{50}) evoking half-maximal estrogenic activity in transcription activation, the dissociation inhibition constants (K_i) calculated from the IC_{50} values of the ES2 displacement curves (Fig. 1), and the corresponding K_i values calculated using the 6D-QSAR model are compared. For Polysantol and Javanol, only the K_i values for the energetically most favorable conformation are reported. The IC_{50} values for the remaining stereoisomers are as follows: 140 ± 173 μM Polysantol (*S,S*), 216 ± 122 μM Polysantol (*S,R*), 2.86 ± 4.45 mM Polysantol (*R,R*), 2.41 ± 2.64 mM Javanol (*R,S*), 176.7 ± 567 μM Javanol (*S,S*), and 40.73 ± 23.33 μM Javanol (*S,R*). The K_i values for the remaining stereoisomeric forms are as follows: 299 μM Polysantol (*S,S*), 83 μM Polysantol (*S,R*), 1 mM Polysantol (*R,R*), 931 μM Javanol (*R,S*), 68 μM Javanol (*S,S*), and 15 μM Javanol (*S,R*).

Compound	EC_{50} of ER activation	K_i of ER competitive binding	K_i of ER predicted
Estradiol	0.16 ± 0.01 nM	1.6 ± 1 nM	2 nM
MC	86 ± 8 μM	76 ± 6 μM	21 μM
Polysantol (*R,S*)[a]	98 ± 23 μM	56 ± 5 μM	26 μM
Javanol (*R,R*)[a]	50 ± 4 μM	ca. 50 μM	5 μM
Androstenol	52 ± 3 μM	ca. 25 μM	10 μM

[a] The indicated stereoisomers were used for predicting K_i values, whereas experiments were performed using mixtures of stereoisomers.

VOLUME 283 (2008) PAGES 36211–36220
DOI 10.1074/jbc.A806576200

TRAF6 and MEKK1 play a pivotal role in the RIG-I-like helicase antiviral pathway.

Ryoko Yoshida, Giichi Takaesu, Hideyuki Yoshida, Fuyuki Okamoto, Tomoko Yoshioka, Yongwon Choi, Shizuo Akira, Taro Kawai, Akihiko Yoshimura, and Takashi Kobayashi

On page 36212, the sequences of PCR primers of IFN-α are incorrect. The correct sequences are as follows: IFN-α, 5′-ATGGCTAGGCTCTGTGCTTTCCT-3′ and 5′-AGGGCTCTCCAGACTTCTGCTCTG-3′.

VOLUME 283 (2008) PAGES 7470–7479
DOI 10.1074/jbc.A707758200

Lysophosphatidic acid receptor-dependent secondary effects via astrocytes promote neuronal differentiation.

Tânia Cristina de Sampaio e Spohr, Ji Woong Choi, Shannon E. Gardell, Deron R. Herr, Stevens Kastrup Rehen, Flávia Carvalho Alcantara Gomes, and Jerold Chun

The first author in the PubMed citation should be listed as Spohr, T. C. S.

VOLUME 283 (2008) PAGES 17881–17890
DOI 10.1074/jbc.A801481200

Biogenesis of MalF and the $MalFGK_2$ maltose transport complex in *Escherichia coli* requires YidC.

Samuel Wagner, Ovidiu Ioan Pop, Gert-Jan Haan, Louise Baars, Gregory Koningstein, Mirjam M. Klepsch, Pierre Genevaux, Joen Luirink, and Jan-Willem de Gier

Dr. Pop's first name was misspelled. His correct name is shown above.

VOLUME 284 (2009) PAGES 11425–11435
DOI 10.1074/jbc.A806395200

MEK1 binds directly to βarrestin1, influencing both its phosphorylation by ERK and the timing of its isoprenaline-stimulated internalization.

Dong Meng, Martin J. Lynch, Elaine Huston, Michael Beyermann, Jenny Eichhorst, David R. Adams, Enno Klussmann, Miles D. Houslay, and George S. Baillie

Dr. Klussmann's name was misspelled. The correct spelling is shown above.